

Journal of Visualized Experiments

Plasma-assisted molecular beam epitaxy growth of Mg₃N₂ and Zn₃N₂ thin films

--Manuscript Draft--

Article Type:	Methods Article - Author Produced Video
Manuscript Number:	JoVE59415R2
Full Title:	Plasma-assisted molecular beam epitaxy growth of Mg ₃ N ₂ and Zn ₃ N ₂ thin films
Keywords:	Plasma-assisted molecular beam epitaxy; II3-V2 semiconductors; Zn ₃ N ₂ ; Mg ₃ N ₂ ; optical growth monitoring; metal effusion cells
Corresponding Author:	Thomas Tiedje University of Victoria Victoria, British Columbia CANADA
Corresponding Author's Institution:	University of Victoria
Corresponding Author E-Mail:	ttiedje@uvic.ca; pengwubuaa@gmail.com
Order of Authors:	Peng Wu Thomas Tiedje
Additional Information:	
Question	Response
Please indicate whether this article will be Standard Access or Open Access.	Standard Access (US\$1200)

TITLE:

Plasma-Assisted Molecular Beam Epitaxy Growth of Mg_3N_2 and Zn_3N_2 Thin Films

AUTHORS & AFFILIATIONS:

Peng Wu¹, Thomas Tiedje¹

¹Department of Electrical and Computer Engineering, University of Victoria, Victoria, British Columbia, Canada

Corresponding Author:

Thomas Tiedje (ttiedje@uvic.ca)

E-mail Address of Co-Author:

Peng Wu (pengwubuaa@gmail.com)

KEYWORDS:

plasma-assisted molecular beam epitaxy, $\text{II}_3\text{-V}_2$ semiconductors, Zn_3N_2 , Mg_3N_2 , optical growth monitoring, metal effusion cells

SUMMARY:

This article describes the growth of epitaxial films of Mg_3N_2 and Zn_3N_2 on MgO substrates by plasma-assisted molecular beam epitaxy with N_2 gas as the nitrogen source and optical growth monitoring.

ABSTRACT:

This article describes a procedure for growing Mg_3N_2 and Zn_3N_2 films by plasma-assisted molecular beam epitaxy (MBE). The films are grown on 100 oriented MgO substrates with N_2 gas as the nitrogen source. The method for preparing the substrates and the MBE growth process are described. The orientation and crystalline order of the substrate and film surface are monitored by the reflection high energy electron diffraction (RHEED) before and during growth. The specular reflectivity of the sample surface is measured during growth with an Ar-ion laser with a wavelength of 488 nm. By fitting the time dependence of the reflectivity to a mathematical model, the refractive index, optical extinction coefficient, and growth rate of the film are determined. The metal fluxes are measured independently as a function of the effusion cell temperatures using a quartz crystal monitor. Typical growth rates are 0.028 nm/s at growth temperatures of 150 °C and 330 °C for Mg_3N_2 and Zn_3N_2 films, respectively.

INTRODUCTION:

The $\text{II}_3\text{-V}_2$ materials are a class of semiconductors that have received relatively little attention from the semiconductor research community compared to III-V and II-VI semiconductors¹. The Mg and Zn nitrides, Mg_3N_2 and Zn_3N_2 , are attractive for consumer applications because they are composed of abundant and non-toxic elements, making them inexpensive and easy to recycle unlike most III-V and II-VI compound semiconductors. They display an anti-bixbyite crystal structure similar to the CaF_2 structure, with one of the interpenetrating fcc F-sublattices being

half-occupied²⁻⁵. They are both direct band gap materials⁶, making them suitable for optical applications⁷⁻⁹. The band gap of Mg_3N_2 is in the visible spectrum (2.5 eV)¹⁰, and the band gap of Zn_3N_2 is in the near-infrared (1.25 eV)¹¹. To explore the physical properties of these materials and their potential for electronic and optical device applications, it is critical to obtain high quality, single crystal films. Most work on these materials to date has been carried out on powders or polycrystalline films made by reactive sputtering¹²⁻¹⁷.

Molecular beam epitaxy (MBE) is a well-developed and versatile method for growing single-crystal compound semiconductor films¹⁸ that has the potential to yield high quality materials using a clean environment and high-purity elemental sources. Meanwhile, MBE rapid shutter action enables changes to a film at the atomic layer scale and allows for precise thickness control. This paper reports on the growth of Mg_3N_2 and Zn_3N_2 epitaxial films on MgO substrates by plasma-assisted MBE, using high purity Zn and Mg as vapor sources and N_2 gas as the nitrogen source.

PROTOCOL:

1. MgO substrate preparation

NOTE: Commercial one-side epi-polished (100) oriented single crystal MgO square substrates (1 cm x 1 cm) were employed for the X_3N_2 (X = Zn and Mg) thin film growth.

1.1 High temperature annealing

1.1.1 Place the MgO on a clean sapphire wafer sample carrier with the polished side facing upwards in a furnace and anneal for 9 h at 1,000 °C. Raise the temperature to 1000 °C over a 10 min period.

NOTE: High temperature annealing removes carbon from the surface and reconstructs the surface crystal structure of the MgO single crystal substrates.

1.1.2 Cool the MgO substrates to the room temperature (RT).

1.2 Substrate cleaning

1.2.1 Collect the annealed MgO substrates and rinse in deionized water in a clean borosilicate glass beaker.

1.2.2 Boil the MgO substrates in 100 mL of acetone in a 250 mL borosilicate glass beaker for 30 min to remove inorganic carbon contamination from handling.

NOTE: Cover the beaker and do not allow the acetone to boil dry.

1.2.3 Drain the acetone and rinse the MgO substrates in 50 mL of methanol.

1.2.4 Blow-dry the substrates with nitrogen gas, then store the dry, clean substrates in the clean chip tray.

2. Operation of VG V80 MBE

2.1 Open the cooling water for the preparation chamber, cryoshroud on the growth chamber (see **Figure 1**), effusion cells, and quartz crystal microbalance sensor.

2.2 Turn on the Ar-ion laser with a wavelength of 488 nm. The laser light is brought to the MBE chamber with an optical fiber from the laser, which is located in another room.

2.3 Turn on the reflection high energy electron diffraction gun (RHEED), 13.56 Mhz radio frequency (rf) plasma generator, and quartz crystal microbalance (QCM) system.

3. Substrate loading

3.1 Fast entry lock

3.1.1 Mount a clean MgO substrate on the molybdenum sample holder (**Figure 2A**) using tungsten spring clips.

3.1.2 Turn off the turbo pump on the fast entry lock (FEL) and vent the FEL chamber with nitrogen. Open the FEL when the chamber pressure reaches atmospheric pressure.

3.1.3 Remove the sampler holder cassette out of the FEL and load the sample holder with the substrate into the cassette.

3.1.4 Load the cassette back into the FEL and turn the turbo pump back on.

3.1.5 Wait for the pressure in the FEL to drop to 10^{-6} Torr.

3.1.6 Increase the temperature of the fast entry lock to 100 °C over a period of 5 min and degas the substrates with the holders for 30 min in the fast entry lock.

3.2 Make sure the pressure in the fast entry lock is below 10^{-7} Torr before opening the vacuum valve to the preparation chamber. Transfer the holder using the wobble stick transfer mechanism to the preparation chamber, then ramp up the degassing station to 400 °C and allow it to degas for 5 h.

3.3 Transfer the degassed holder by the trolley transfer mechanism to the sample manipulator in the growth chamber. Increase the substrate temperature up to 750 °C over a period of 30 min and allow the sample to outgas in the manipulator for another 30 min. Make sure the cooling water is turned on in the cryoshroud to avoid overheating the cryoshroud.

3.4 Drop the temperature of the substrate to 150 °C for Zn₃N₂ film growth and 330 °C for Mg₃N₂ film growth using the thermocouple in the sample manipulator to measure the sample temperature.

3.5 In-situ RHEED

3.5.1 Set the voltage on the electron gun to 15 kV and filament current to 1.5 A once the growth chamber pressure is below 1×10^{-7} Torr.

3.5.2 Rotate the substrate holder until 1) the electron gun is aligned along a principle crystallographic axis of the substrate and 2) a clear single crystal electron diffraction pattern is visible.

3.5.3 Take a picture of the RHEED pattern and save the picture.

3.6 Close the shutter on the effusion cell and stop the flow of nitrogen. Measure the RHEED pattern for the deposited film when the chamber pressure is below 10^{-7} Torr.

4. Metal flux measurements

4.1 Use standard group III type effusion cells or low temperature effusion cells for Mg and Zn.

4.2 Load the crucibles with 15 g and 25 g of high purity Mg and Zn shot, respectively.

4.3 When the growth chamber has achieved a vacuum of 10^{-8} Torr or better, and before loading the substrate holder, outgas the Zn or Mg source effusion cells up to 250 °C at a ramp rate of ~20 °C/min and allow it to outgas for 1 h with the shutters closed.

4.4 After the substrate has been loaded into the sample manipulator, heat the Zn and/or Mg effusion cells to 350 °C or 390 °C respectively, at a ramp rate of ~10 °C/min, and wait 10 min for them to stabilize with the shutters closed.

4.5 Use the retractable quartz crystal monitor to measure the metal flux. Position the quartz crystal sensor in front of the substrate inside the chamber. Make sure the substrate is fully covered by the detector so that no metal is deposited on the substrate.

4.6 Input the density of the metal of interest ($\rho_{\text{Zn}} = 7.14 \text{ g/cm}^3$, $\rho_{\text{Mg}} = 1.74 \text{ g/cm}^3$) into the quartz crystal monitor (QCM) controller.

4.7 To calibrate the flux, open the shutter for one of the metal sources and allow the effusion cell to deposit on the sensor. The QCM system converts its internal measurement of mass to thickness.

4.8 Calculate the elemental flux from the slope of the increasing thickness as a function of time shown on the QCM. The rate of increase of the thickness over a few minutes is proportional to the elemental flux. In two example cases, a Zn flux of 0.45 nm/s and a Mg flux of 1.0 nm/s are obtained.

4.9 Change the temperature of the effusion cells and repeat step 4.8 if the temperature dependence of the flux is required. The measured temperature dependence of the Mg and Zn flux is shown in **Figure 3** for this specific growth system.

4.10 When the flux measurements are complete, close the shutters on the effusion cells and retract the quartz crystal sensor.

5. Nitrogen plasma

5.1 Turn off the filament current and high voltage on the RHEED gun to prevent damage in the presence of a high N₂ gas pressure in the growth chamber.

5.2 Open the gas valve on the high pressure N₂ cylinder.

5.3 Slowly open the leak valve slowly until the nitrogen pressure in the growth chamber reaches 3×10^{-5} – 4×10^{-5} Torr.

5.4 Set the power of the plasma generator to 300 W.

5.5 Ignite the plasma with the ignitor on the plasma source. A bright purple glow will be visible from the viewport when the plasma ignites, as shown in **Figure 2B**.

5.6 Adjust the control on the rf matching box to minimize the reflected power as much as possible. A reflected power of less than 15 W is good; in this case, the reflected power is reduced to 12 W.

6. In situ laser light scattering

6.1 Focus the chopped 488 nm Argon laser light reflected from the substrate in the growth chamber onto the Si photodiode so that an electrical signal can be detected by the lock-in amplifier. This is accomplished by adjusting the angle of the substrate by rotating the substrate holder around two axes and adjusting the position of the Si detector, then focusing the lens that collects the reflected light as shown in **Figure 4**.

6.2 Open the shutter of one of the metal sources.

6.3 Record the time-dependent reflectivity with a computer-controlled data logger. The growth of an epitaxial film will produce an oscillatory reflected signal with time associated with thin film optical interference between the front and back surfaces of the film.

6.4 To protect the film from oxidation in air, deposit an encapsulation layer to protect the film from oxidation in air. This is especially important for Mg_3N_2 which oxidizes rapidly in air.

6.5 In order to deposit a MgO encapsulation layer, close the nitrogen gas, switch to oxygen gas, repeat step 5.3, and increase the oxygen pressure to 1×10^{-5} Torr.

6.6 Set the power of the plasma generator to 250 W and repeat step 5.5. The plasma starts at lower rf power with oxygen gas than with nitrogen gas.

6.7 Open the shutter on the Mg source, and repeat step 6.4 for 5–10 min.

NOTE: This will produce a MgO film that is about 10 nm thick. The uncapped Mg_3N_2 films are yellow but fade quickly to a whitish color within 20 s upon exposure to air. Consequently, an encapsulation layer is required to allow time for measurements on the films before they oxidize after removal from the vacuum chamber.

6.8 Close the gas valves, turn off the laser, and ramp down the substrate and cell temperatures to $\sim 25^\circ\text{C}$ in 30 min. Turn off the cooling water and the rf power to the plasma source.

6.9 After several growth runs, the optical windows become covered with metal. Remove the metal by wrapping the window in aluminum foil and heating it with heating tape to 400°C and a temperature ramp rate of $\sim 15^\circ\text{C}/\text{min}$ or slower over the course of a weekend.

7. Growth rate determination

7.1 Use **Equation 1** below to describe the optical reflectivity of the sample^{11,19}.

$$\mathcal{R} = RR^* = \frac{r_1^2 + r_2^2 e^{-4\alpha(t)} + 2r_1 r_2 e^{-2\alpha} \cos(2\delta_1(t))}{1 + r_1^2 r_2^2 e^{-4\alpha(t)} + 2r_1 r_2 e^{-2\alpha} \cos(2\delta_1(t))} \quad (1)$$

Where:

$$r_1 = \frac{1-n_1}{1+n_1} \quad (1 - a)$$

$$r_2 = \frac{n_1-n_2}{n_1+n_2} \quad (1 - b)$$

$$\delta_1(t) = \frac{2\pi}{\lambda} n_1 g t \left[1 - \left(\frac{\sin \theta_0}{n_1} \right)^2 \right]^{1/2} \quad (1 - c)$$

$$\alpha(t) = \frac{2\pi}{\lambda} k_1 g t \left[1 - \left(\frac{\sin \theta_0}{n_1} \right)^2 \right]^{1/2} \quad (1 - d)$$

And where: $n_2 = 1.747$ is the refractive index of the MgO substrate at a wavelength of 488 nm; θ_0 is the angle of the incident beam measured with respect to the substrate surface normal; and t is time. The optical constants of the film (n_1 and k_1) and growth rate (g) are obtained by fitting the reflectivity as a function of time in **Equation 1**.

REPRESENTATIVE RESULTS:

The black object in the inset in **Figure 5B** is a photograph of an as-grown 200 nm Zn_3N_2 thin film. Similarly, the yellow object in the inset in **Figure 5C** is an as-grown 220 nm Mg_3N_2 thin film. The yellow film is transparent to the extent that it is easy-to-read text placed behind the film¹⁰.

The surface of the substrate and the films were monitored *in situ* by RHEED. **Figure 5A** shows the RHEED pattern of a bare substrate with the electron beam incident along the [110] direction of the substrate. RHEED patterns for the deposited films in **Figure 5B,C** show that the crystal lattices of the Zn_3N_2 and Mg_3N_2 thin films are oriented in the plane of the substrate surface, as expected in the case of epitaxial growth. The disadvantage of RHEED for growth monitoring under the conditions used here is that the growth process must be stopped to allow the pressure to drop to 10^{-7} Torr and turn on the electron gun.

In contrast with RHEED, *in situ* optical reflectivity measurements are not affected by pressure in the chamber. To obtain the growth rate, *in situ* optical reflectivity was fit as a function of time shown in **Figure 6** using **Equation 1**. In this equation, growth time t is the independent variable, and the optical constants of the film (n_1 , k_1) and growth rate g are fitting parameters. In **Figure 6**, the MgO substrate refractive index, angle of incidence, and wavelength are $n_2 = 1.747$, $\theta_0 = 36.5^\circ$, and $\lambda = 488$ nm, respectively. The fitted refractive index of the film is $n_1 = 2.65$, extinction coefficient is $k_1 = 0.54$, and growth rate is $g = 0.031$ nm/s for the Zn_3N_2 thin film as shown in **Figure 6A**. Similarly, the best fit refractive index for the Mg_3N_2 film is $n_1 = 2.4$, extinction coefficient is $k_1 = 0.09$, and growth rate is $g = 0.033$ nm/s as shown in **Figure 6B**. The overall decrease in the specular reflection with time in **Figure 6B** is believed to be caused by an increase in surface roughness scattering as the Mg_3N_2 thin film becomes thicker. The effect of the roughness scattering was simulated by multiplying the calculated reflectivity with a decaying exponential, $e^{-\beta t}$, where $\beta = 8 \times 10^{-5} \text{ s}^{-1}$ and the growth time t is measured in seconds.

Upon exposure to air, the uncapped yellow Mg_3N_2 films faded within minutes to a translucent white color. On the other hand, the Mg_3N_2 films that were capped with MgO were relatively stable. To further protect the capped Mg_3N_2 films from oxidation, the $\text{Mg}_3\text{N}_2/\text{MgO}$ heterostructures were coated with a CaF_2 layer deposited by electron beam evaporation. Uncapped Zn_3N_2 is more stable; however, the initially black Zn_3N_2 films also oxidized over time and turned grey within a few months. The oxidation reaction is believed to involve the formation of magnesium hydroxide and release ammonia according to the following chemical reaction²⁰. A ZnO layer deposited using a similar method to the MgO can also be used as a protective layer to prevent oxidation.

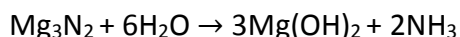


FIGURE LEGENDS:

Figure 1: View of the VG V80H molecular beam epitaxy growth chamber. This picture shows the MBE growth chamber with (clockwise) the RHEED screen and camera housing, quadrupole residual gas analyzer, optical hardware on laser light scattering port, Mg effusion cell, N-plasma source, rf matching box, and the Zn effusion cell.

Figure 2: Substrate holder and glow from plasma source. (A) Molybdenum sample holder plate with two tungsten wire clips holding the square MgO substrate in place. (B) Purple glow originating from the back window of the plasma source when operating with N₂ gas.

Figure 3: Metal flux as a function of effusion cell temperature. The lines are fit to the temperature dependence of the metal fluxes using an Arrhenius relation as discussed in the text.

Figure 4: Schematic of the in-situ laser light scattering setup.

Figure 5: RHEED patterns. (A) RHEED diffraction pattern for MgO substrate. (B) RHEED pattern of as-grown Zn₃N₂ film with photograph of black Zn₃N₂ film. (C) RHEED pattern of as-grown Mg₃N₂ substrate with photograph of yellow Mg₃N₂ film.

Figure 6: In situ specular reflectivity. In situ specular reflectivity at 488 nm of (A) Zn₃N₂ and (B) Mg₃N₂ films during growth. The calculated reflectivity (red line) is best-fit to the experimental data (blue circles) as discussed in the text.

DISCUSSION:

A variety of considerations is involved in the choice of substrates and establishing the growth conditions that optimize the structural and electronic properties of the films. The MgO substrates are heated at high temperature in air (1000 °C) to remove carbon contamination from the surface and improve the crystalline order in the substrate surface. Ultrasonic cleaning in acetone is a good alternative method to clean the MgO substrates.

The (400) X-ray diffraction peak for the Zn₃N₂ films was found to be narrower when the film was grown on high-temperature, annealed MgO substrates compared to when grown on unannealed substrates. The lattice constant of MgO (0.421 nm) is significantly smaller than (half of) the lattice constant of Zn₃N₂ (0.976 nm) or Mg₃N₂ (0.995 nm) and not well-matched to the semiconductor films. The lattice constants of the commercially available groups IV, III-V, and II-VI substrates are all larger than the lattice constants of Mg₃N₂ and Zn₃N₂. A more well-matched substrate is desirable. Silicon, which has a lattice constant of 0.543 nm, is somewhat more well-matched to Mg₃N₂ than MgO and is worth to be explored. Zn₃N₂ films were also grown on A-plane sapphire substrates. The structural quality of these films was not as good as that seen in the MgO substrates, as indicated by the RHEED spots and width of the (400) Zn₃N₂ X-ray

diffraction peak. In the case of the sapphire substrates, the backside was coated with Cr (50 nm) and Mo (200 nm) to improve thermal coupling between the substrate holder and substrate.

The substrate temperature is measured during growth with a thermocouple located in the enclosed vacuum space between the substrate holder and heater, and it is not in physical contact with the substrate holder or the substrate. As a result, it was expected that the actual substrate temperature would be lower than the sensor temperature. Successful Mg_3N_2 and Zn_3N_2 growths were obtained with thermocouple temperatures in the 300–350 °C and 140–180 °C ranges, respectively.

High growth temperature increases the mobility of the ad-atoms on the growing surface and may be expected to produce material with fewer structural defects. However, at high substrate temperatures, the growth rate is lower, which is interpreted as being due to re-evaporation of metal atoms from the surface. At high metal flux, film growth rate is limited by the supply of active nitrogen. The active nitrogen is maximized at high rf power applied to the plasma source (300 W max) and at a high nitrogen flow rate. The N_2 flow rate is limited by the maximum pressure in the growth chamber, which in this case was in the mid 10^{-5} Torr range. Ammonia is a possible alternative nitrogen source. Mg and Zn will react with NH_3 at a high temperature without plasma activation; however, it is unclear whether the residence time of Mg and Zn atoms on the surface will be long enough to support film growth at temperatures for which NH_3 will react with the metals.

In these experiments, effusion cells were used with pyrolytic boron nitride (PBN) crucibles with capacities of 40 cc for Mg and 25 cc for Zn. **Figure 3** shows the temperature dependence of the Mg and Zn fluxes from the effusion cells. The straight lines in **Figure 3** are fit to the measured temperature dependence of the fluxes. The fits have the form $\text{Flux} = A \exp(-B/kT)$, and the fitting parameters (A,B) are (8.5×10^{17} nm/s, 2.3 eV) and (1.3×10^{15} nm/s, 1.9 eV) for the Mg and Zn sources, respectively. The flux approximately doubles with each 10 °C and 12 °C increase in the effusion cell temperature for Mg and Zn, respectively. For the growth illustrated in **Figure 6**, the metal fluxes were near the maxima in **Figure 3** (~1 nm/s with Mg flux higher than Zn flux) but the film growth rates were only 0.03 nm/s. This shows that the metal utilization efficiency is low, with Mg being lower than Zn and most of the metal re-evaporating.

The high N_2 background pressure during growth precludes the continuous monitoring of the film growth with RHEED. Differential pumping of the RHEED gun can solve this problem. *In situ* optical reflectivity measurements serve as a complementary monitoring tool that is not affected by gas pressure and provides an accurate and reliable technique for determining the growth rate. The non-specular or diffuse reflectivity of the substrate can also be measured *in situ* and will provide information on surface roughness during growth.

The base pressure in the MBE growth chamber is 10^{-8} Torr with the N_2 gas turned off. The cryoshroud in the growth chamber is cooled with water during film growth. Under these conditions, some residual oxygen contamination can be expected in the films. The residual

water vapour pressure in the growth chamber can be reduced with a lower temperature coolant in the shroud, such as silicone oil at -80 °C²¹.

In conclusion, this protocol describes how to grow single crystal films of Mg₃N₂ and Zn₃N₂ by plasma-assisted molecular beam epitaxy and provides suggestions for how the growth process can be changed to further improve film quality. These materials did not show photoluminescence at either room temperature or a low temperature. There is a need to make a further defect density in the films. Mg₃N₂-Zn₃N₂ alloys can also be grown by plasma-assisted molecular beam epitaxy.

ACKNOWLEDGMENTS:

This work was supported by the Natural Sciences and Engineering Research Council of Canada.

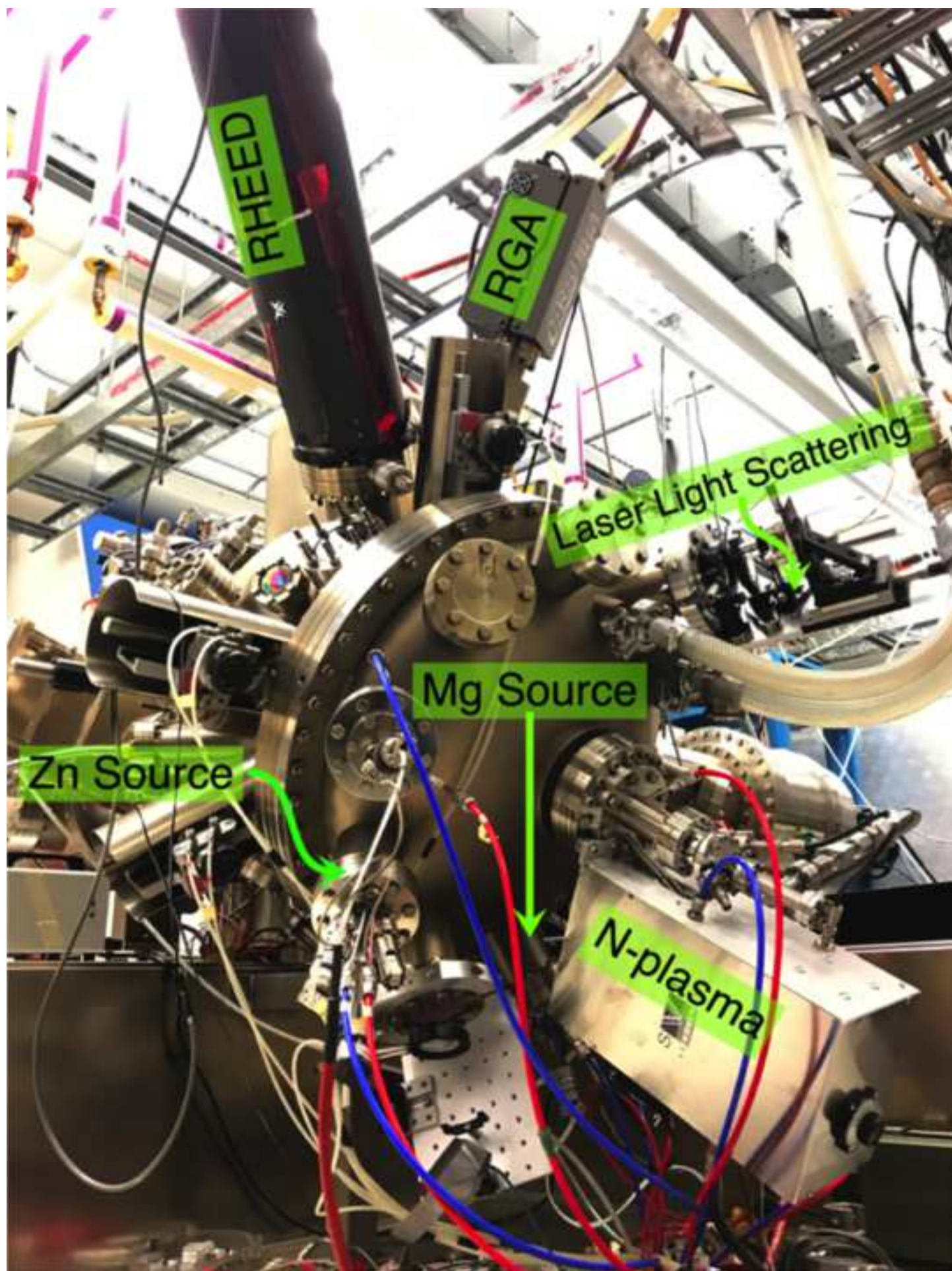
DISCLOSURES:

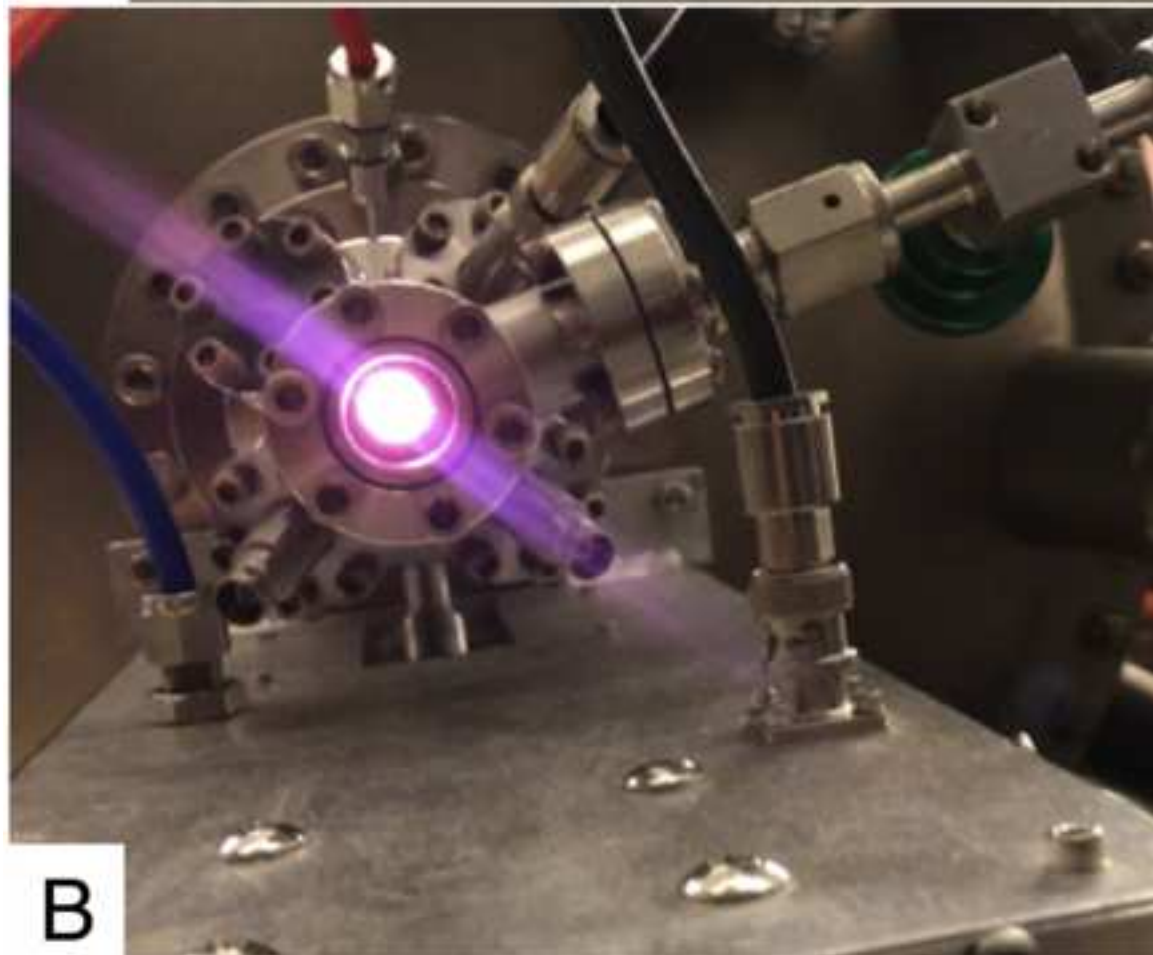
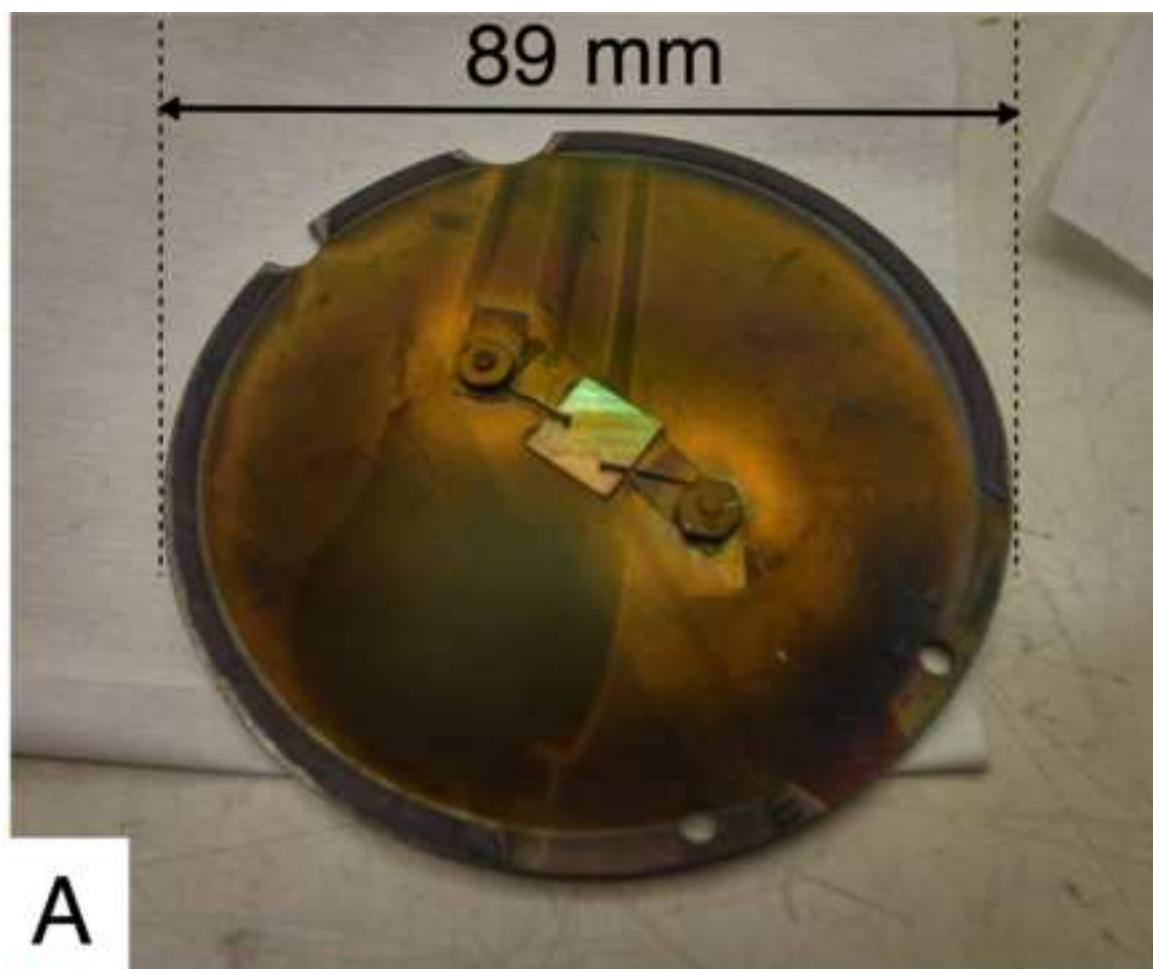
The authors have nothing to disclose.

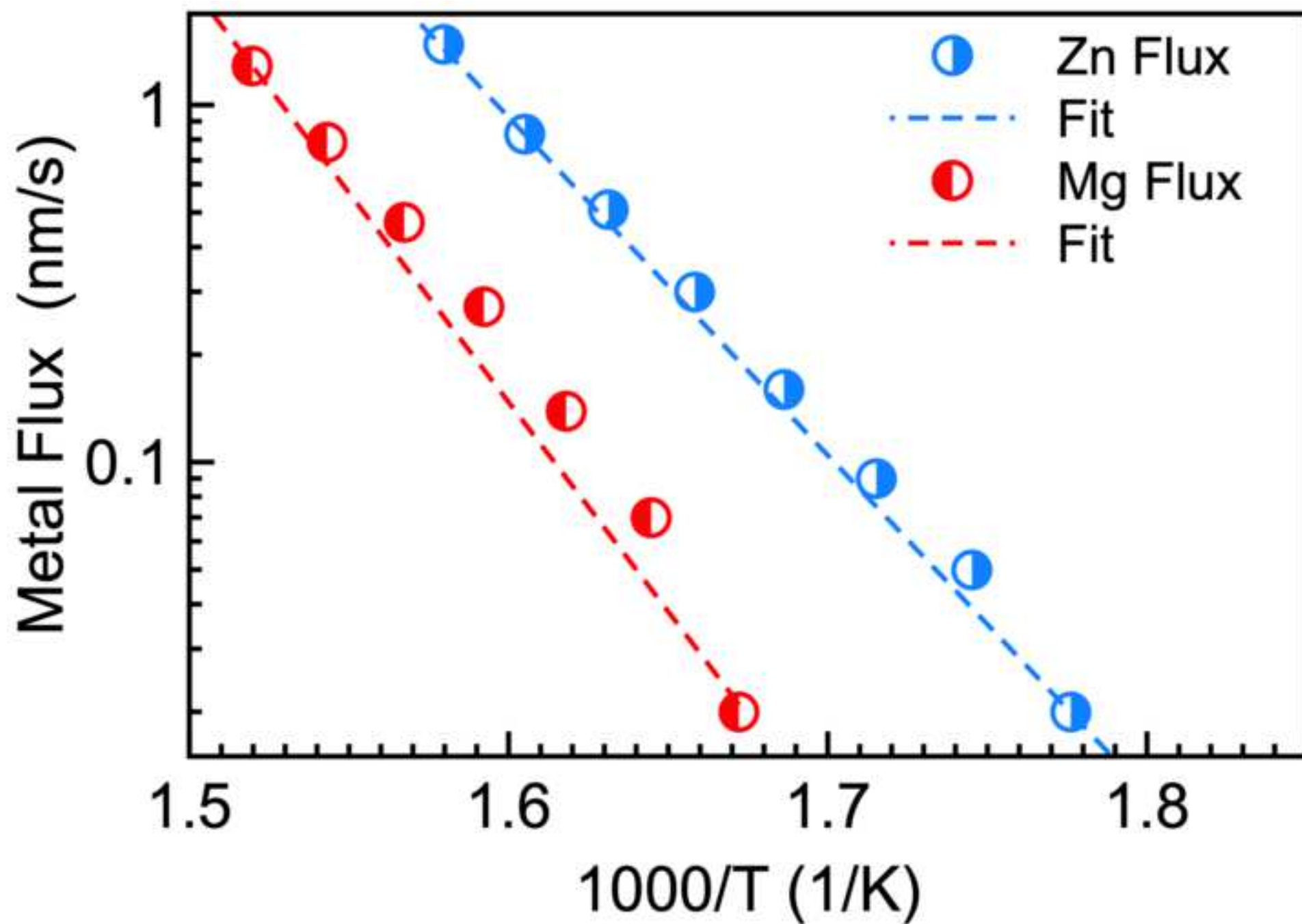
REFERENCES:

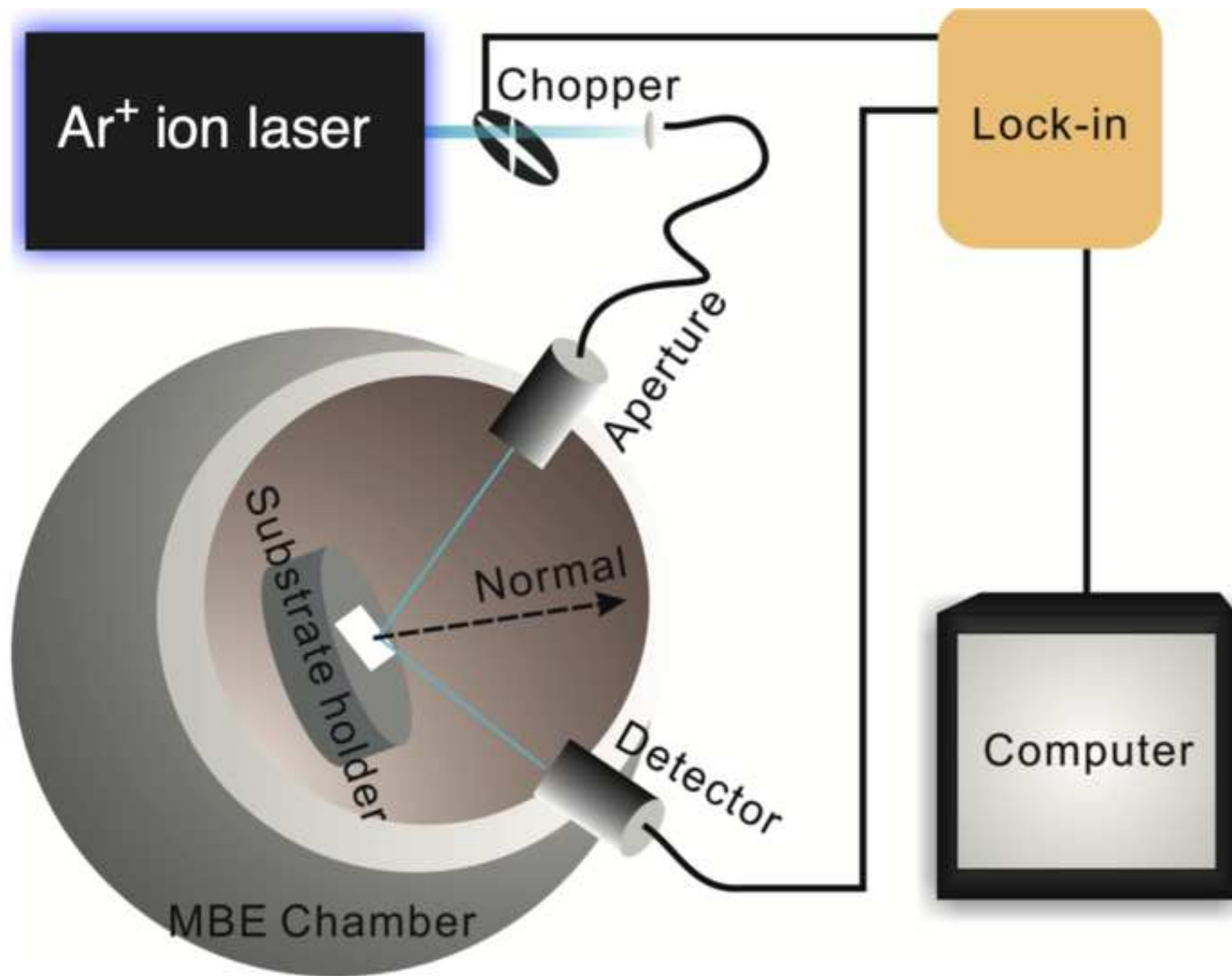
1. Suda, T., Kakishita, K. Band-gap energy and electron effective mass of polycrystalline Zn₃N₂. *Journal of Applied Physics*. **99** (7), 076101.1-076101.3 (2006).
2. Hu, J., Bando, Y., Zhan, J., Zhi, C., Golberg, D. Carbon nanotubes as nanoreactors for fabrication of single-crystalline Mg₃N₂ nanowires. *Nano Letters*. **6** (6), 1136-1140 (2006).
3. Fang, C. M., Groot, R. A., Bruls, R. J., Hintzen, H. T., With, G. Ab initio band structure calculations of Mg₃N₂ and MgSiN₂. *Journal of Physics: Condensed Matter*. **11** (25), 4833-4842 (1999).
4. Yoo, S. H., Walsh, A., Scanlon, D. O., Soon, A. Electronic structure and band alignment of zinc nitride, Zn₃N₂. *RSC Advances*. **4** (7), 3306-3311 (2014).
5. Partin, D. E., Williams, D. J., O'Keeffe, M. The crystal structures of Mg₃N₂ and Zn₃N₂. *Journal of Solid-State Chemistry*. **132** (1), 56-59 (1997).
6. Ullah, M., Murtaza, G., Ramay, S. M., Mahmood, A. Structural, electronic, optical and thermoelectric properties of Mg₃X₂ (X = N, P, As, Sb, Bi) compounds. *Materials Research Bulletin*. **91**, 22-30 (2017).
7. Li, C. T. et. al. Electrocatalytic zinc composites as the efficient counter electrodes of dye-sensitized solar cells: study on the electrochemical performance and density functional theory Calculations. *ACS Applied Materials & Interfaces*. **7** (51), 28254-28263 (2015).
8. Sinha, S., Choudhury, D., Rajaraman, G., Sarkar, S. Atomic layer deposition of Zn₃N₂ thin films: growth mechanism and application in thin film transistor. *RSC Advances*. **5** (29), 22712–22717 (2015).
9. Bhattacharyya, S. R., Ayouchi, R., Pinnisch, M., Schwarz, R. Transfer characteristic of zinc nitride based thin film transistors. *Physica Status Solidi C*. **9** (3-4), 469–472 (2012).
10. Wu, P., Tiedje, T. Molecular beam epitaxy growth and optical properties of Mg₃N₂ films. *Applied Physics Letters*. **113** (8), 082101.1-082101.4 (2018).
11. Wu, P. et al. Molecular beam epitaxy growth and optical properties of single crystal Zn₃N₂ films. *Semiconductor Science and Technology*. **31** (10), 10LT01.1-10LT01.4 (2016).

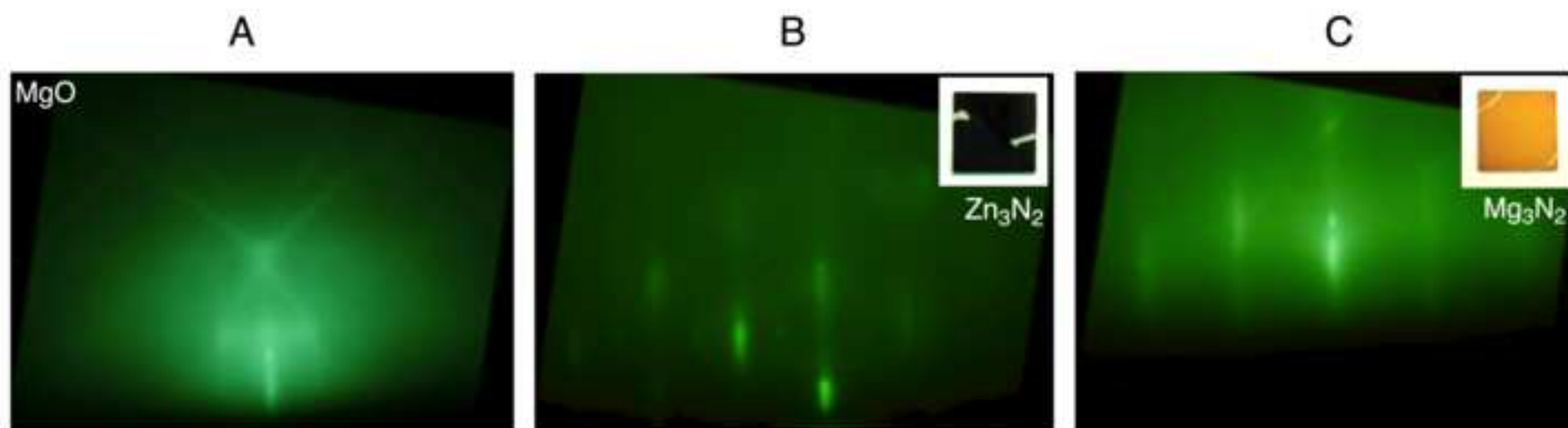
12. Jiang, N., Georgiev, D. G., Jayatissa, A. H. The effects of the pressure and the oxygen content of the sputtering gas on the structure and the properties of zinc oxy-nitride thin films deposited by reactive sputtering of zinc. *Semiconductor Science and Technology*. **28** (2), 025009 (2013).
13. Nakano, Y., Morikawa, T., Ohwaki, T., Taga, Y. Electrical characterization of p-type N-doped ZnO films prepared by thermal oxidation of sputtered Zn₃N₂ films. *Applied Physics Letters*. **88** (17), 172103.1-172103.3 (2006).
14. Cao, X., Yamaguchi, Y., Ninomiya, Y., Yamada, N. Comparative study of electron transport mechanisms in epitaxial and polycrystalline zinc nitride films. *Journal of Applied Physics*. **119** (2), 025104.1-025104.10 (2016).
15. Jia, J., Kamijo, H., Nakamura, S., Shigesato, Y. How the sputtering process influence structural, optical, and electrical properties of Zn₃N₂ films. *MRS Communications*. **8** (2), 314-321 (2018).
16. Trapalis, A., Hefferman, J., Farrer, I., Sherman, J., Kean, A. Structural, electrical and optical characterization of as-grown and oxidized zinc nitride films. *Journal of Applied Physics*. **120** (20), 205102.1-205102.9 (2016).
17. Núñez, C. G. et al. On the zinc nitride properties and the unintentional incorporation of oxygen. *Thin Solid Films*. **520** (6), 1924-1929 (2012).
18. Oshima, T., Fujita, S. (111)-oriented Zn₃N₂ growth on a-plane sapphire substrates by molecular beam epitaxy. *Japanese Journal of Applied Physics*. **45** (11), 8653–8655 (2006).
19. Heavens, O. S. *Optical properties of thin solid films*. Butterworth, London, 46-48 (1955).
20. Heyns, A. H., Prinsloo, L. C., Range, K. -J., Stassen, M. The vibrational spectra and decomposition of α -calcium nitride (α -Ca₃N₂) and magnesium nitride (Mg₃N₂). *Journal of Solid-State Chemistry*. **137**, 33-41 (1998).
21. Lewis, R. B., Bahrami-Yekta, V., Patel, M. J., Tiedje, T., Masnadi-Shirazi, M. Closed-cycle cooling of cryopanel in molecular beam epitaxy. *Journal of Vacuum Science Technology B*. **32** (2) 02C102.1-02C102.7 (2014).

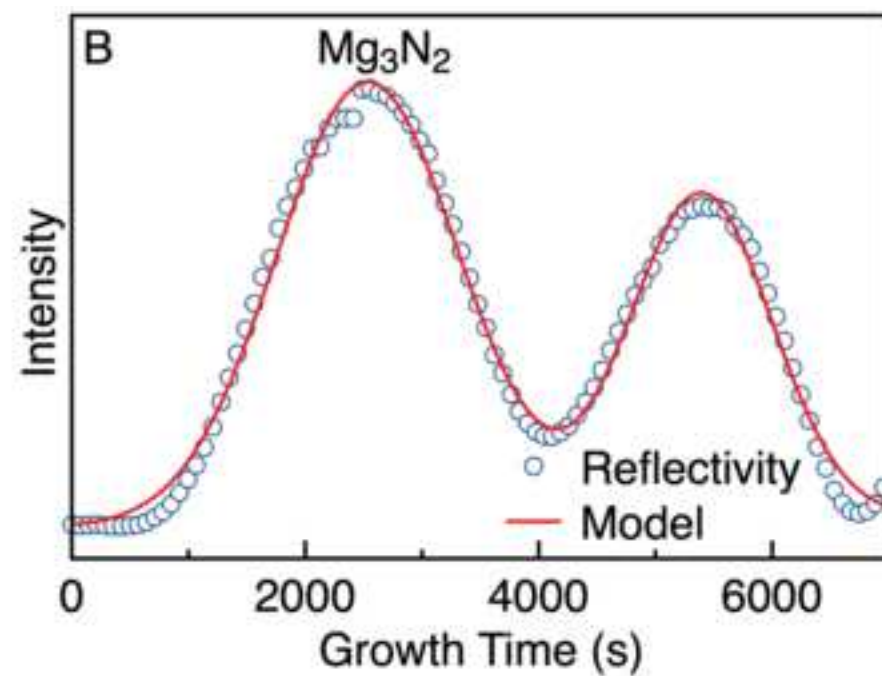
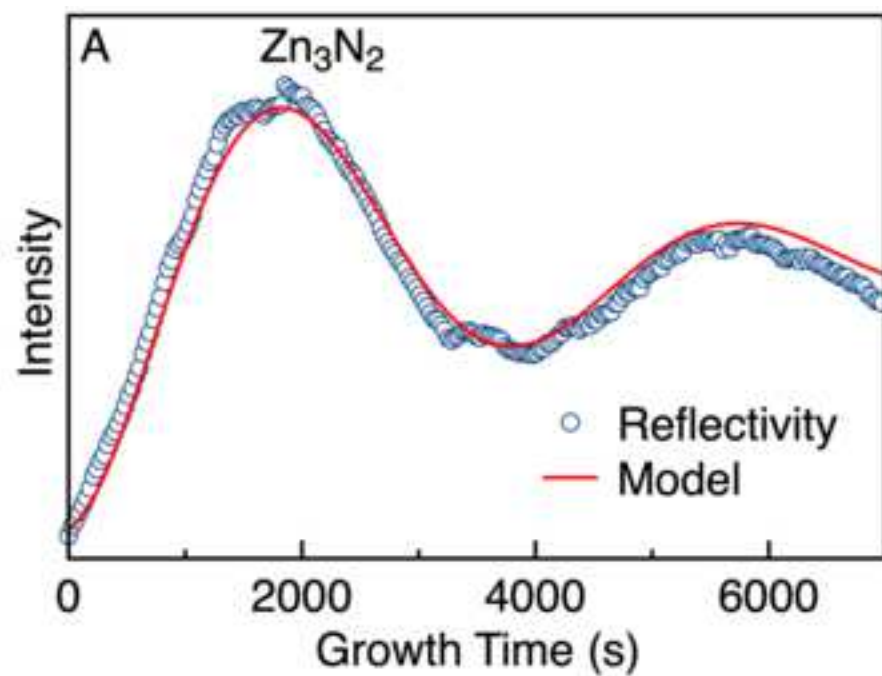












Name of Material/ Equipment	Company	Catalog Number	Comments/Description
(100) MgO	University Wafer	214018	one side epi-polished
Acetone	Fisher Chemical	170239	99.8%
Argon laser	Lexel Laser	00-137-124	488 nm visible wavelength, 350 mW output power
Chopper	Stanford Research system	SR540	Max. Frequency: 3.7 kHz
Lock-in amplifier	Stanford Research system	37909	DSP SR810, Max. Frequency: 100 kHz
Magnesium	UMC	MG6P5	99.9999%
MBE system	VG Semicon	V80H0016-2 SHT 1	V80H-10
Methanol	Alfa Aesar	L30U027	Semi-grade 99.9%
Nitrogen	Praxair	402219501	99.998%
Oxygen	Linde Gas	200-14-00067	> 99.9999%
Plasma source	SVT Associates	SVTA-RF-4.5PBN	PBN, 0.11" Aperture, Specify Length: 12" – 20"
Si photodiode	Newport	2718	818-UV Enhanced, 200 - 1100 nm
Zinc	Alfa Aesar	7440-66-6	99.9999%



1 Alewife Center #200
Cambridge, MA 02140
tel. 617.945.9051
www.jove.com

ARTICLE AND VIDEO LICENSE AGREEMENT

Title of Article:

Molecular beam epitaxy growth of X₃N₂(X=Zn and Mg) thin films

Author(s):

Peng Wu, and Thomas Tiedje

Item 1 (check one box): The Author elects to have the Materials be made available (as described at

<http://www.jove.com/author>) via: ☒ Standard Access ☐ Open Access

Item 2 (check one box):

- ☒ The Author is NOT a United States government employee.
- ☐ The Author is a United States government employee and the Materials were prepared in the course of his or her duties as a United States government employee.
- ☐ The Author is a United States government employee but the Materials were NOT prepared in the course of his or her duties as a United States government employee.

ARTICLE AND VIDEO LICENSE AGREEMENT

1. **Defined Terms.** As used in this Article and Video License Agreement, the following terms shall have the following meanings: “**Agreement**” means this Article and Video License Agreement; “**Article**” means the article specified on the last page of this Agreement, including any associated materials such as texts, figures, tables, artwork, abstracts, or summaries contained therein; “**Author**” means the author who is a signatory to this Agreement; “**Collective Work**” means a work, such as a periodical issue, anthology or encyclopedia, in which the Materials in their entirety in unmodified form, along with a number of other contributions, constituting separate and independent works in themselves, are assembled into a collective whole; “**CRC License**” means the Creative Commons Attribution-Non Commercial-No Derivs 3.0 Unported Agreement, the terms and conditions of which can be found at: <http://creativecommons.org/licenses/by-nc-nd/3.0/legalcode>; “**Derivative Work**” means a work based upon the Materials or upon the Materials and other pre-existing works, such as a translation, musical arrangement, dramatization, fictionalization, motion picture version, sound recording, art reproduction, abridgment, condensation, or any other form in which the Materials may be recast, transformed, or adapted; “**Institution**” means the institution, listed on the last page of this Agreement, by which the Author was employed at the time of the creation of the Materials; “**JoVE**” means MyJoVE Corporation, a Massachusetts corporation and the publisher of *The Journal of Visualized Experiments*; “**Materials**” means the Article and / or the Video; “**Parties**” means the Author and JoVE; “**Video**” means any video(s) made by the Author, alone or in conjunction with any other parties, or by JoVE or its affiliates or agents, individually or in collaboration with the Author or any other parties, incorporating all or any portion of the Article, and in which the Author may or may not appear.

2. **Background.** The Author, who is the author of the Article, in order to ensure the dissemination and protection of the Article, desires to have the JoVE publish the Article and create and transmit videos based on the Article. In furtherance of such goals, the Parties desire to memorialize in this Agreement the respective rights of each Party in and to the Article and the Video.

3. **Grant of Rights in Article.** In consideration of JoVE agreeing to publish the Article, the Author hereby grants to JoVE, subject to **Sections 4** and **7** below, the exclusive, royalty-free, perpetual (for the full term of copyright in the Article, including any extensions thereto) license (a) to publish, reproduce, distribute, display and store the Article in all forms, formats and media whether now known or hereafter developed (including without limitation in print, digital and electronic form) throughout the world, (b) to translate the Article into other languages, create adaptations, summaries or extracts of the Article or other Derivative Works (including, without limitation, the Video) or Collective Works based on all or any portion of the Article and exercise all of the rights set forth in (a) above in such translations, adaptations, summaries, extracts, Derivative Works or Collective Works and (c) to license others to do any or all of the above. The foregoing rights may be exercised in all media and formats, whether now known or hereafter devised, and include the right to make such modifications as are technically necessary to exercise the rights in other media and formats. If the “Open Access” box has been checked in **Item 1** above, JoVE and the Author hereby grant to the public all such rights in the Article as provided in, but subject to all limitations and requirements set forth in, the CRC License.

ARTICLE AND VIDEO LICENSE AGREEMENT

4. Retention of Rights in Article. Notwithstanding the exclusive license granted to JoVE in **Section 3** above, the Author shall, with respect to the Article, retain the non-exclusive right to use all or part of the Article for the non-commercial purpose of giving lectures, presentations or teaching classes, and to post a copy of the Article on the Institution's website or the Author's personal website, in each case provided that a link to the Article on the JoVE website is provided and notice of JoVE's copyright in the Article is included. All non-copyright intellectual property rights in and to the Article, such as patent rights, shall remain with the Author.

5. Grant of Rights in Video – Standard Access. This **Section 5** applies if the "Standard Access" box has been checked in **Item 1** above or if no box has been checked in **Item 1** above. In consideration of JoVE agreeing to produce, display or otherwise assist with the Video, the Author hereby acknowledges and agrees that, Subject to **Section 7** below, JoVE is and shall be the sole and exclusive owner of all rights of any nature, including, without limitation, all copyrights, in and to the Video. To the extent that, by law, the Author is deemed, now or at any time in the future, to have any rights of any nature in or to the Video, the Author hereby disclaims all such rights and transfers all such rights to JoVE.

6. Grant of Rights in Video – Open Access. This **Section 6** applies only if the "Open Access" box has been checked in **Item 1** above. In consideration of JoVE agreeing to produce, display or otherwise assist with the Video, the Author hereby grants to JoVE, subject to **Section 7** below, the exclusive, royalty-free, perpetual (for the full term of copyright in the Article, including any extensions thereto) license (a) to publish, reproduce, distribute, display and store the Video in all forms, formats and media whether now known or hereafter developed (including without limitation in print, digital and electronic form) throughout the world, (b) to translate the Video into other languages, create adaptations, summaries or extracts of the Video or other Derivative Works or Collective Works based on all or any portion of the Video and exercise all of the rights set forth in (a) above in such translations, adaptations, summaries, extracts, Derivative Works or Collective Works and (c) to license others to do any or all of the above. The foregoing rights may be exercised in all media and formats, whether now known or hereafter devised, and include the right to make such modifications as are technically necessary to exercise the rights in other media and formats. For any Video to which this Section 6 is applicable, JoVE and the Author hereby grant to the public all such rights in the Video as provided in, but subject to all limitations and requirements set forth in, the CRC License.

7. Government Employees. If the Author is a United States government employee and the Article was prepared in the course of his or her duties as a United States government employee, as indicated in **Item 2** above, and any of the licenses or grants granted by the Author hereunder exceed the scope of the 17 U.S.C. 403, then the rights granted hereunder shall be limited to the maximum rights permitted under such

statute. In such case, all provisions contained herein that are not in conflict with such statute shall remain in full force and effect, and all provisions contained herein that do so conflict shall be deemed to be amended so as to provide to JoVE the maximum rights permissible within such statute.

8. Protection of the Work. The Author(s) authorize JoVE to take steps in the Author(s) name and on their behalf if JoVE believes some third party could be infringing or might infringe the copyright of either the Author's Article and/or Video.

9. Likeness, Privacy, Personality. The Author hereby grants JoVE the right to use the Author's name, voice, likeness, picture, photograph, image, biography and performance in any way, commercial or otherwise, in connection with the Materials and the sale, promotion and distribution thereof. The Author hereby waives any and all rights he or she may have, relating to his or her appearance in the Video or otherwise relating to the Materials, under all applicable privacy, likeness, personality or similar laws.

10. Author Warranties. The Author represents and warrants that the Article is original, that it has not been published, that the copyright interest is owned by the Author (or, if more than one author is listed at the beginning of this Agreement, by such authors collectively) and has not been assigned, licensed, or otherwise transferred to any other party. The Author represents and warrants that the author(s) listed at the top of this Agreement are the only authors of the Materials. If more than one author is listed at the top of this Agreement and if any such author has not entered into a separate Article and Video License Agreement with JoVE relating to the Materials, the Author represents and warrants that the Author has been authorized by each of the other such authors to execute this Agreement on his or her behalf and to bind him or her with respect to the terms of this Agreement as if each of them had been a party hereto as an Author. The Author warrants that the use, reproduction, distribution, public or private performance or display, and/or modification of all or any portion of the Materials does not and will not violate, infringe and/or misappropriate the patent, trademark, intellectual property or other rights of any third party. The Author represents and warrants that it has and will continue to comply with all government, institutional and other regulations, including, without limitation all institutional, laboratory, hospital, ethical, human and animal treatment, privacy, and all other rules, regulations, laws, procedures or guidelines, applicable to the Materials, and that all research involving human and animal subjects has been approved by the Author's relevant institutional review board.

11. JoVE Discretion. If the Author requests the assistance of JoVE in producing the Video in the Author's facility, the Author shall ensure that the presence of JoVE employees, agents or independent contractors is in accordance with the relevant regulations of the Author's institution. If more than one author is listed at the beginning of this Agreement, JoVE may, in its sole discretion, elect not take any action with respect to the Article until such time as it has received complete, executed Article and Video License Agreements from each such author. JoVE reserves the right, in its absolute and sole discretion and without giving any reason therefore, to accept or decline any work submitted to JoVE. JoVE and its employees, agents and independent contractors shall have

ARTICLE AND VIDEO LICENSE AGREEMENT

full, unfettered access to the facilities of the Author or of the Author's institution as necessary to make the Video, whether actually published or not. JoVE has sole discretion as to the method of making and publishing the Materials, including, without limitation, to all decisions regarding editing, lighting, filming, timing of publication, if any, length, quality, content and the like.

11. **Indemnification.** The Author agrees to indemnify JoVE and/or its successors and assigns from and against any and all claims, costs, and expenses, including attorney's fees, arising out of any breach of any warranty or other representations contained herein. The Author further agrees to indemnify and hold harmless JoVE from and against any and all claims, costs, and expenses, including attorney's fees, resulting from the breach by the Author of any representation or warranty contained herein or from allegations or instances of violation of intellectual property rights, damage to the Author's or the Author's institution's facilities, fraud, libel, defamation, research, equipment, experiments, property damage, personal injury, violations of institutional, laboratory, hospital, ethical, human and animal treatment, privacy or other rules, regulations, laws, procedures or guidelines, liabilities and other losses or damages related in any way to the submission of work to JoVE, making of videos by JoVE, or publication in JoVE or elsewhere by JoVE. The Author shall be responsible for, and shall hold JoVE harmless from, damages caused by lack of sterilization, lack of cleanliness or by contamination due to the making of a video by JoVE its employees, agents or independent contractors. All sterilization, cleanliness or decontamination procedures shall be solely the responsibility of the Author and shall be undertaken at the Author's

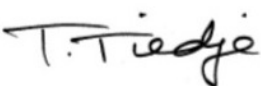
expense. All indemnifications provided herein shall include JoVE's attorney's fees and costs related to said losses or damages. Such indemnification and holding harmless shall include such losses or damages incurred by, or in connection with, acts or omissions of JoVE, its employees, agents or independent contractors.

12. **Fees.** To cover the cost incurred for publication, JoVE must receive payment before production and publication the Materials. Payment is due in 21 days of invoice. Should the Materials not be published due to an editorial or production decision, these funds will be returned to the Author. Withdrawal by the Author of any submitted Materials after final peer review approval will result in a US\$1,200 fee to cover pre-production expenses incurred by JoVE. If payment is not received by the completion of filming, production and publication of the Materials will be suspended until payment is received.

13. **Transfer, Governing Law.** This Agreement may be assigned by JoVE and shall inure to the benefits of any of JoVE's successors and assignees. This Agreement shall be governed and construed by the internal laws of the Commonwealth of Massachusetts without giving effect to any conflict of law provision thereunder. This Agreement may be executed in counterparts, each of which shall be deemed an original, but all of which together shall be deemed to be one and the same agreement. A signed copy of this Agreement delivered by facsimile, e-mail or other means of electronic transmission shall be deemed to have the same legal effect as delivery of an original signed copy of this Agreement.

A signed copy of this document must be sent with all new submissions. Only one Agreement required per submission.

CORRESPONDING AUTHOR:

Name:	Thomas Tiedje	
Department:	Electrical and Computer Engineering	
Institution:	University of Victoria	
Article Title:	Molecular beam epitaxy growth of X ₃ N ₂ (X=Zn and Mg) thin films	
Signature:		Date: Nov. 19, 2018

Please submit a signed and dated copy of this license by one of the following three methods:

- 1) Upload a scanned copy of the document as a pdf on the JoVE submission site;
- 2) Fax the document to +1.866.381.2236;
- 3) Mail the document to JoVE / Attn: JoVE Editorial / 1 Alewife Center #200 / Cambridge, MA 02139

For questions, please email submissions@jove.com or call +1.617.945.9051

Responses to the editorial comments:

1. The editor has formatted the manuscript to match the journal's style. Please retain the same.

OK

2. Please address all the specific comments marked in the manuscript.

Done

3. If any of the figures are previously published, please obtain explicit copyright permission to reuse any figures from a previous publication. Explicit permission can be expressed in the form of a letter from the editor or a link to the editorial policy that allows re-prints. Please upload this information as a .doc or .docx file to your Editorial Manager account. The Figure must be cited appropriately in Figure Legend, i.e. "This figure has been modified from [citation]."

All figures are original figures and not previously published

Changes in the Video:

1. Please increase the homogeneity between the written protocol and the narration in the video. Essentially, it would be best if the narration is a word for word from the written protocol text.

We have brought the narration into closer alignment with the written protocol by re-recording the sections of the video described below.

Time 1: 1:54-2:53

Protocol: Open the cooling water for the preparation chamber, the cryoshroud on the growth chamber (see Fig.1), the effusion cells, and the quartz crystal microbalance sensor. Turn on the Ar ion laser with a wavelength of 488 nm. The laser light is brought to the MBE chamber with an optical fiber from the laser which is located in another room. Turn on the reflection high-energy electron diffraction gun (RHEED), 13.56 Mhz radio frequency (rf) plasma generator, and quartz crystal microbalance (QCM) system. Mount a clean MgO substrate on the molybdenum sample holder (Fig. 2A) using the tungsten spring clips. Turn off the turbo pump on the fast entry lock (FEL) and vent the FEL chamber with nitrogen.

New voice over: The first step in the MBE growth is to turn the cooling water on, this is the water on the effusion cells, then we turn on the growth monitoring laser, RHEED power supply, the RF plasma generator power supply and the quartz crystal microbalance system. MgO substrates are mounted on 3" diameter molybdenum sample holders with tungsten spring clips. The first step in loading the samples into the MBE is to turn off the turbo pump and vent the fast entry lock.

Old voice over: The first step in the MBE growth is to turn the water on, this is the water on the effusion cells, then we turn on the growth monitoring laser, RHEED power supply, the RF power supply and the crystal growth monitor.

MgO substrates are mounted on 3" diameter molybdenum sample holders with tungsten spring clips. The first step in loading the samples into the MBE is to vent the fast entry lock.

Time 2: 4:10-4:35

Protocol: Standard group-III type effusion cells or low temperature effusion cells were used for Mg and Zn. The crucibles were loaded with 15 g and 25 g of high purity (6-9's) Mg and Zn shot, respectively. When the growth chamber has achieved a vacuum of 10^{-8} Torr or better and before loading the substrate holder, heat the Zn or Mg source effusion cells up to 250 °C at a ramp rate of ~ 20 °C/min and allow to outgas for one hour.

New voice over: Standard group-III type effusion cells or low temperature effusion cells were used for Mg and Zn. The crucibles were loaded with 15 g and 25 g of high purity Mg and Zn shot, respectively. The Zn and Mg source effusion cells are outgassed at 250 degrees C for one hour with their shutters closed.

Old voice over: The Zn and Mg source effusion cells are outgassed at 250 degrees C for one hour with their shutters closed.

Time 3: 5:15-5:22

Protocol: Input the density of the metal of interest ($\rho_{\text{Zn}} = 7.14 \text{ g/cm}^3$, $\rho_{\text{Mg}} = 1.74 \text{ g/cm}^3$) into the quartz crystal monitor (QCM) controller.

New voice over: Input the density of the metal into the quartz crystal monitor (QCM) controller.

Old voice over: The density of the Zn and Mg is programmed into the quartz crystal controller

Time 4: 6:22-6:32

Protocol: Turn off the filament current and the high voltage on the RHEED gun to prevent damage in the presence of a high N_2 gas pressure in the growth chamber.

New voice over: Turn off the filament current and the high voltage on the RHEED gun to prevent damage in the presence of a high N_2 gas pressure in the growth chamber.

Old voice over: no voice over in old version

Time 5: 7:23-8:34

Protocol: Focus the chopped 488 nm Argon laser light reflected from the substrate in the growth chamber onto the Si photodiode so that an electrical signal can be detected by the

lock-in amplifier. This is accomplished by adjusting the angle of the substrate by rotating the substrate holder around two axes and by adjusting the position of the Si detector and focusing lens that collects the reflected light as shown in Fig. 4. Open the shutter of one of the metal sources. Record the time dependent reflectivity with a computer-controlled data logger. The growth of an epitaxial film will produce an oscillatory reflected signal with time associated with thin film optical interference between the front and back surfaces of the film

New voice over: Focus the chopped 488 nm Argon laser light reflected from the substrate in the growth chamber onto the Si photodiode so that an electrical signal can be detected by the lock-in amplifier. This is accomplished by adjusting the angle of the substrate by rotating the substrate holder around two axes and by adjusting the position of the Si detector and focusing lens that collects the reflected light as shown in this picture. Open the shutter of one of the metal sources. Record the time dependent reflectivity with a computer-controlled data logger. The growth of an epitaxial film will produce an oscillatory reflected signal with time associated with thin film optical interference between the front and back surfaces of the film.

Old voice over: The light from a mechanically chopped argon ion laser is transported to the MBE system with an optical fiber. The light from the optical fiber is focused through a window in the growth chamber onto the substrate. The reflected light is picked up by a silicon photodiode at a specular window located on the opposite side of the growth chamber. A laser line filter is used to block all the light except the 488 nm light from the argon laser. The photodiode output is measured with a lock-in amplifier and this signal is proportional to the reflectivity of the surface of the substrate. The reflectance shows slow oscillations as the film grows due to thin film interference between the front and back of the film.

Time 6: 9:03-9:18

Protocol: In order to deposit a MgO encapsulation layer, close the nitrogen gas, and switch to oxygen gas, repeat (5.3) and increase the oxygen pressure to 1×10^{-5} Torr.

New voice over: In order to deposit a MgO encapsulation layer, close the nitrogen gas, and switch to oxygen gas and increase the oxygen pressure to 1×10^{-5} Torr.

Old voice over: no voice over in old version

2. 1:18. *There is a break in the audio, the sentence is incomplete and ends in "with". Please edit this part.*

Corrected

3. 2:17-2:18. *The VO is cut here as well. Please edit this part.*

Corrected

4. 4:10: *This part of the VO needs to be redone as well.*

Corrected

5. 10:51-11:50 - *The audio and video appear to be slightly out of sync here. This should be corrected.*

Corrected

6. *After all the formatting, please ensure that the video file cannot exceed 15 min in length.*

13 min in total

Figures 1-6

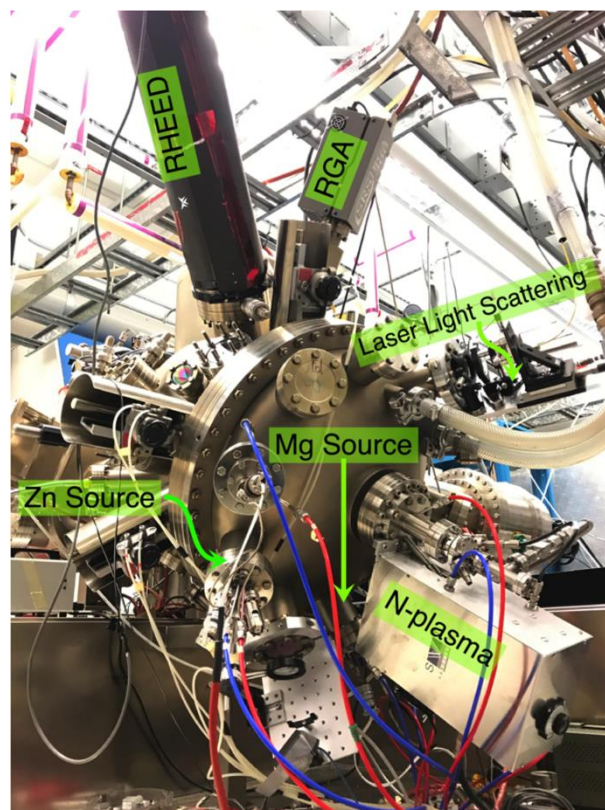


Figure 1. View of the VG V80H molecular beam epitaxy growth chamber. The clockwise showing the RHEED screen and camera housing, quadrupole residual gas analyzer, optical hardware on laser light scattering port, Mg effusion cell, N-plasma source and rf matching box, and the Zn effusions cell.

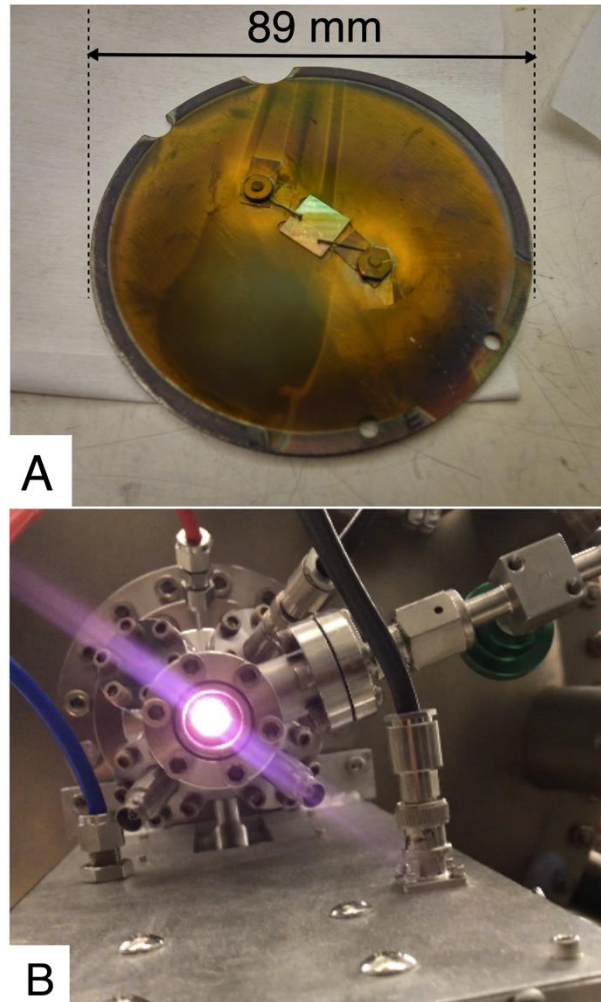


Figure 2. MBE components. A. molybdenum sample holder plate, with two tungsten wire clips used to hold the MgO substrate in place (square object) and **B.** view of the purple glow coming from the back window of the N2-plasma source when it is in operation.

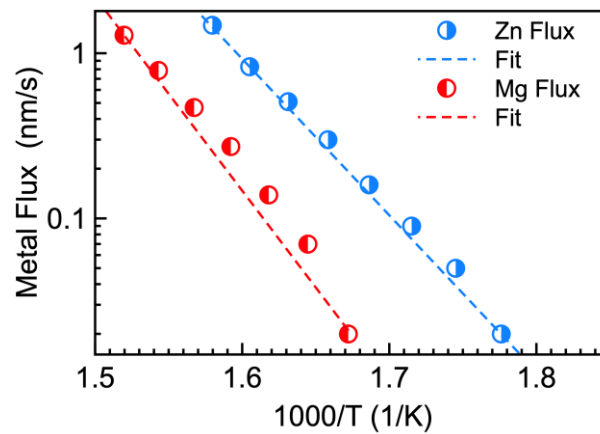


Figure 3. Metal flux as a function of effusion cell temperature.

20

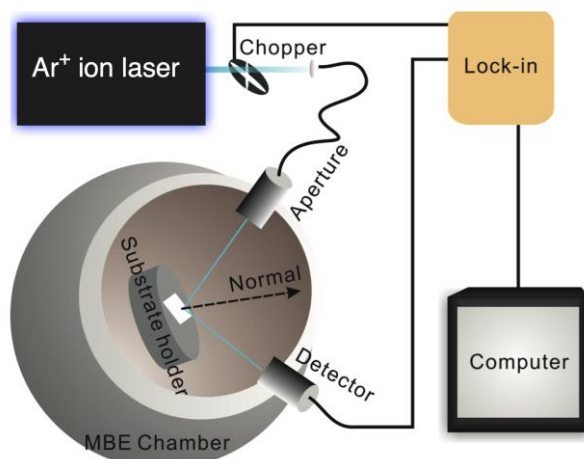


Figure 4. Schematics of the in-situ laser light scattering setup.

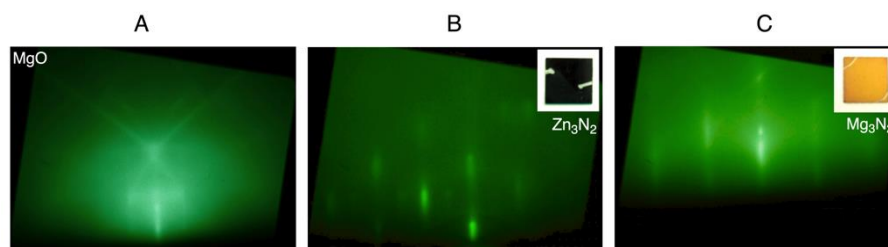


Figure 5. RHEED patterns. **A.** RHEED pattern of MgO substrate. **B.** RHEED pattern of as-grown Zn_3N_2 film with photograph of black Zn_3N_2 film. **C.** RHEED pattern of as-grown Mg_3N_2 substrate with photograph of yellow Mg_3N_2 film.

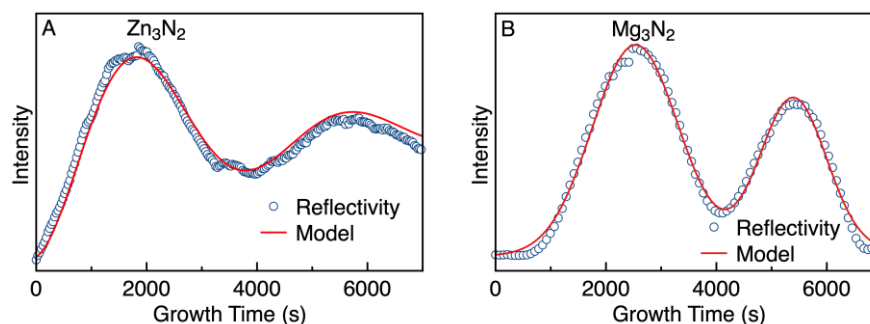


Figure 6. In situ specular reflectivity. In situ specular reflectivity at 488 nm of **A.** Zn_3N_2 and **B.** Mg_3N_2 films. The calculated reflectivity (red line) is a best fit to the experimental data (blue circles) as discussed in the text.